

## Ozone Generation in Corona Discharge at Pin Electrode of Electrophotographic Charger\*

H. Kawamoto<sup>▲</sup>

Department of Mechanical Engineering, Waseda University, Shinjyuku, Tokyo, Japan

The generation of ozone in a stable regime of DC corona discharge at a pin electrode is modeled to provide data that can be utilized for the evaluation of charging and transferring devices of electrophotography with respect to reducing the ozone emission. The results of a theoretical investigation show the following: (1) The ozone generation rates at a 5 liter/min air flow rate for a 50  $\mu\text{m}$  radius pin electrode are 0.085 ppm/ $\mu\text{A}$  and 0.010 ppm/ $\mu\text{A}$  for negative and positive charging corona, respectively. (2) The ozone generation rate increases with respect to the increase of the pin radius and can be assumed to be linear under normal operation conditions. (3) For positive charging corona, ozone is generated mainly at the surface of the pin electrode, whereas the ozone formation is displaced with a maximum generation rate located at 0.1–0.3 mm from the electrode for negative charging corona. (4) The ozone generation rate for the saw-toothed electrodes is about one-third that of a typical biased charging roller and only 1/140 that of a corotron.

Journal of Imaging Science and Technology 44: 452–456 (2000)

### Introduction

One of the important issues of electrophotography technology is to reduce ozone emitted by charging and transferring devices, such as corotrons, scorotrons<sup>1</sup> or biased contact rollers,<sup>2–5</sup> because not only does ozone damage photoreceptors and consequently causes the deterioration of images, it is also harmful for humans.<sup>6</sup> For this reason, several experimental and theoretical studies have been performed on ozone synthesis in gas discharge field. Nashimoto<sup>7</sup> carried out a parametric experiment on corotrons to investigate the effects of discharge wire and shield materials, wire diameter, and the difference of positive and negative corona. Naidis<sup>8</sup> established an elegant theoretical model that can be used to predict the rate of plasma chemical processes in stable positive and negative corona discharges between the wire and a coaxial cylinder. The author<sup>9</sup> modified Naidis' model to carry out more accurate calculation on ozone emission from the corotron. Because ozone emission from the corotron is still high, biased contact charging roller has been developed as a new charging device to realize extremely low ozone emission.<sup>2–5,10</sup> The system consists of a highly electroresistive elastomer roller and a power supply. DC voltage superposed on AC voltage is applied between the photoreceptor drum and the charger roller.

The electrical micro-discharge in the vicinity of the nip controls the charging of the photoreceptor.<sup>10</sup> Although ozone is also formed in this system due to the electrical discharge, it is extremely small.<sup>11</sup> An ozone filter is usually not necessary to satisfy environmental standards using this charger. Hence it is sometimes termed the virtually ozone free charger. However, a contact charger roller is used only in low-speed machines, for the photoreceptor wears rapidly in this system due to the mechanical contact between the charger roller and the photoreceptor. Alternative discharge current induced by the application of AC voltage accelerates the wear of a photoreceptor, because active ions generated in the vicinity of the contact area attack organic photoconductors. It is believed that the wear mechanism is similar with ion etching. Furthermore, it is difficult to realize uniform charging using this charger for high-speed machines.<sup>10</sup>

Another new ozone-free charger was proposed by Furukawa and co-workers.<sup>12,13</sup> It has saw-tooth electrodes to which DC high voltage is applied through each resistor as schematically shown in Fig. 1. It was confirmed that interposed resistors control sway and dispersion of discharge current from each discharge electrode. Consequently it can uniformly charge the photoreceptor with less discharge current and the amount of generated ozone is less than that of the charging device with parallel-connected saw-tooth electrodes to which high voltage is directly applied. In this study, the author has established a theoretical model to calculate ozone emission from this new device that has a potential to realize an ozone-free charger applicable for high-speed machines. The results of the calculation were compared with experimental results, and some fundamental characteristics and feasibility for the electrophotography charger are discussed.

Original manuscript received December 1, 1999

▲ IS&T Fellow

\* This article has been presented at the International Conference on Digital Printing Technologies (NIP15) at Orlando, Florida in October 20, 1999.

©2000, IS&T—The Society for Imaging Science and Technology

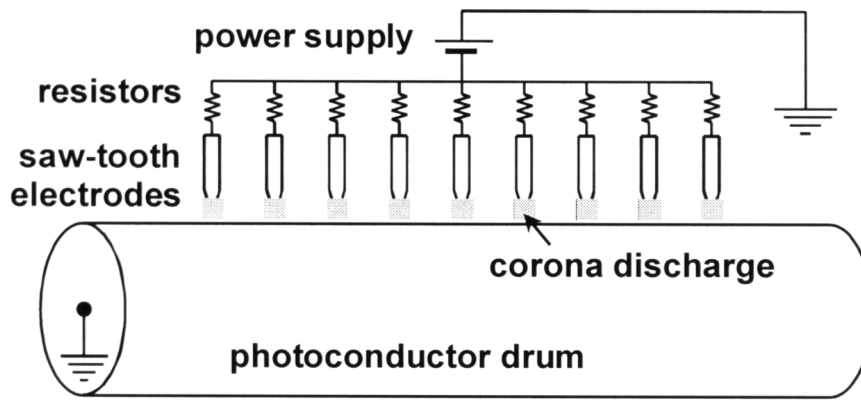


**Figure 1.** Schematic drawing of new charger with parallel-connected saw-tooth electrodes to which high voltage is applied through each resistor.

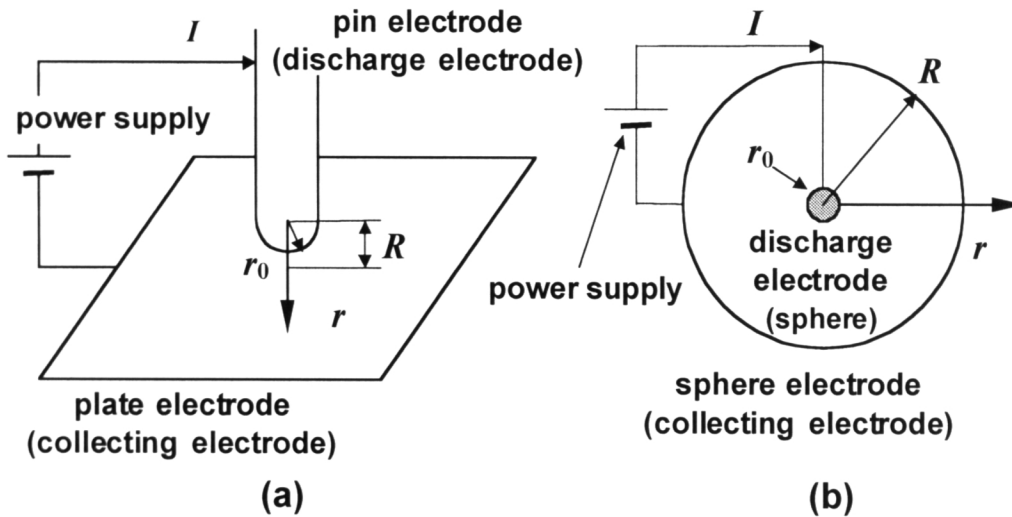


**Figure 2.** Configurations of (a) pin-to-plate electrode and (b) sphere-to-sphere electrode model.

## Modeling

### Ozone Generation Rate in Corona Discharge

The saw-tooth electrode is assumed to be a pin-to-plate system shown in Fig. 2(a). The number density of pin electrodes and cross talks between adjacent electrodes are neglected. It is further simplified to the one-dimensional concentric sphere-to-sphere geometry shown in Fig. 2(b). High voltage, larger than a corona onset voltage, is applied between the inner and the outer sphere. The plasma reaction rate  $W$ , number of ozone molecules generated per unit time, is

$$W_{\pm} = \frac{I}{e} \int_{r_0}^R \psi_{\pm}(r) \alpha_r(r) dr . \quad (1)$$

Here,  $I$  is the total discharge current,  $e$  the charge of an electron,  $R$  the radius of the outer sphere (collecting electrode), and  $r_0$  the radius of the inner sphere (discharge electrode). Subscripts + and - mean positive and negative corona, respectively. Two parameters, the ratio of the electron current and the total current  $\psi$  and the reaction rate constant  $\alpha_r$ , are analytically expressed based on the Townsend theory as a function of the electric field  $E(r)$ .<sup>8,9,11</sup>

$$\alpha_r(r) = An_m \exp\left(-\frac{Bn_m}{E(r)}\right),$$

$$\psi_+(r) = \exp\left(\int_{r_0}^r -\alpha_+(r) dr\right),$$

$$\alpha_+(r) = Cn_m \exp\left(-\frac{Dn_m}{E(r)}\right),$$

$$\psi_-(r) = \gamma \exp\left(\int_{r_0}^r -\alpha_-(r) dr\right),$$

$$\alpha_-(r) = Cn_m \exp\left(-\frac{Dn_m}{E(r)}\right) - Fn_m ,$$

where  $\alpha$  and  $\gamma$  are the first and the second Townsend ionization coefficients,  $\ln(1/\gamma) = 8$ ,  $n_m$  is the concentration of molecular oxygen, and  $A, B, C, D, F$  are experimental constants,  $A = 5.6 \times 10^{-20} \text{ m}^2$ ,  $B = 2.1 \times 10^{-19} \text{ Vm}^2$ ,  $C = 3 \times 10^{-20} \text{ m}^2$ ,  $D = 8 \times 10^{-19} \text{ Vm}^2$ ,  $F = 2 \times 10^{-23} \text{ m}^2$ .<sup>8,14,15</sup> Equation 1 can be numerically integrated using the Simpson's integral method and the ozone concentration  $c$  (ppm) is calculated at a certain air flow rate  $Q$  (liter/min),  $c = 2.23 \times 10^{-15} W/Q$ .

### Distribution of Electric Field

If the discharge current is small and thus there are negligibly small ions and/or electrons in the field, distribution of the electric field is derived from the Laplace equation,<sup>16</sup> i.e.,  $E = E_0(r_0/r)^2$ , where  $E_0 = E(r = r_0) = V/r_0$ . However, because the electric field of corona discharge is determined not only by the electrostatic potential  $\phi$ , but also by the ionic charge density  $\rho$ , the distribution of the electric field deviates from the Laplacian form. The electric field in the discharge field is determined by the conservation law of charge  $\nabla \cdot (-\omega\rho\nabla\phi) = 0$  and Poisson's equation  $\nabla^2\phi = -\rho/\varepsilon_0$  ( $\omega$  is the mobility of ions and  $\varepsilon_0$  is the permittivity of free space), if diffusion and convection of charged particles are neglected and the field is assumed to be unipolar.<sup>16</sup> These two coupled differential equations can be analytically solved in the one-dimensional spherical coordinate under the boundary condition,  $E = E_0$  at  $r = r_0$ .

$$E(r) = E_0 \left( \frac{r_0}{r} \right)^2 \sqrt{1 + \frac{I}{6\pi\varepsilon_0\omega r_0 E_0^2} \left\{ \left( \frac{r}{r_0} \right)^3 - 1 \right\}}. \quad (2)$$

Equation 2 coincides with the Laplacian form in case of no discharge ( $I = 0$ ) but the distribution of the electric field is relaxed under discharge condition.

Because it was experimentally confirmed that the electric field at the surface of the discharge electrode preserves the value determined by the corona ignition voltage,<sup>17</sup> the electric field at the surface of the discharge wire  $E_0$  is calculated by the Naidis' method or Peek's formula.

### Naidis' Method

The electric field at the surface of the discharge electrode is implicitly determined by the following integral equation.<sup>8</sup>

$$\int_{r_0}^R C n_m \exp\left(-\frac{D n_m}{E_0 r_0^2} r^2\right) dr = \ln\left(\frac{1}{\gamma_{ph}}\right),$$

where  $\gamma_{ph}$  is the effective photoionization coefficient [ $\ln(1/\gamma_{ph}) = 8$ ]. Simpson's method was used for numerical integration and simple bisection method was applied to derive  $E_0$  implicitly. It was numerically deduced that  $E_0$  is almost independent of  $R$  and  $I$  at the usual geometry  $R/r_0 > 3$  and the actual operating condition  $I < 50 \mu\text{A}$ .

### Peek's Formula

Peek's formula was experimentally determined from spark ignition voltages in sphere-to-plate systems.<sup>14</sup>

$$E_0 = 27.9\delta \left( 1 + \frac{0.533}{\sqrt{\delta r_0}} \right) \text{ (kV/cm, } r_0: \text{ cm)},$$

where  $\delta$  is a relative air density,  $\delta = 0.386p/(273+T)$ ,  $p$ : pressure (mmHg),  $T$ : temperature ( $^{\circ}\text{C}$ ).

Result of numerical calculation shown in Fig. 3 indicates that calculated results by two methods coincide fairly well with each other. Naidis' method is used in this report.

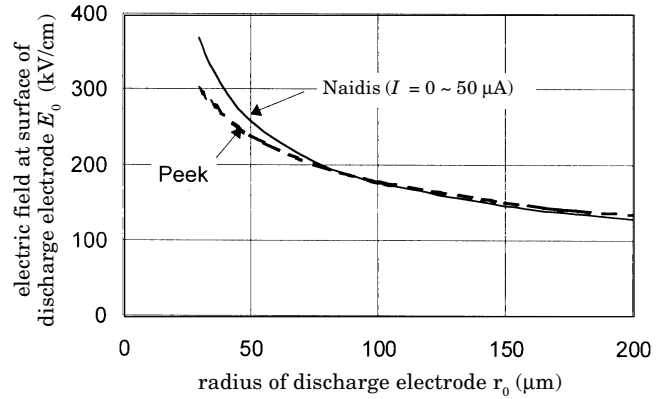


**Figure 3.** Radius of discharge electrode versus electric field at the surface of discharge electrode ( $R = 20 \text{ mm}$ ).

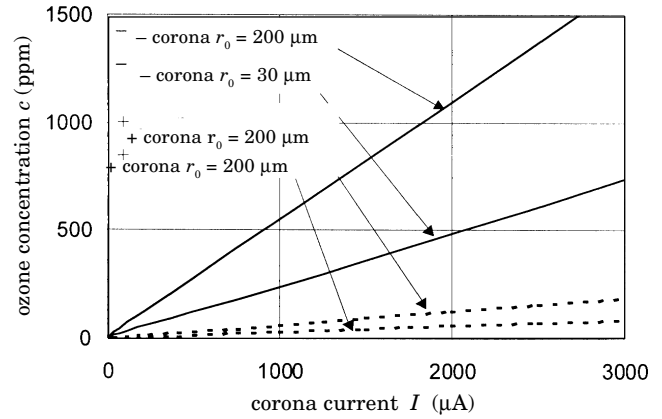


**Figure 4.** Linearity of ozone generation with respect to corona current (calculated,  $Q = 1.5 \text{ liter/min}$ ,  $R = 20 \text{ mm}$ ).

### Effect of Discharge Current

Figure 4 shows the relationship between the discharge current and the calculated ozone concentration. Because the electric field depends on the discharge current, the calculated ozone concentration is not linearly proportional to the discharging current. However, the nonlinearity is negligibly small under actual operating conditions. This characteristic is same as that of the corotron<sup>7,9</sup> and was experimentally confirmed in the pin-to-plate system as reported in Refs. 13, 18 and 19.

### Distribution of Electron Current and Ozone Formation Rate

Figures 5 and 6 show the calculated distributions of the electron current ratio  $\psi_{+,-}(r)$  and the differential ozone formation rate  $\psi_{+,-}(r)\alpha_{+,-}(r)$ , respectively, in positive and negative corona. It is clearly recognized that in the case of the positive corona the electron current is high at the surface of the discharge electrode and ozone is formed just at the surface, because electrons migrate toward the tip of the discharge electrode and are concentrated at the tip. On the contrary, in the negative corona ozone is formed about 0.1 mm away from the discharge electrode. The electron divergence from the negative discharge electrode and the electric field determine the position of the maximum ozone formation rate, which is about 0.1 mm away from a 50  $\mu\text{m}$  diameter discharge

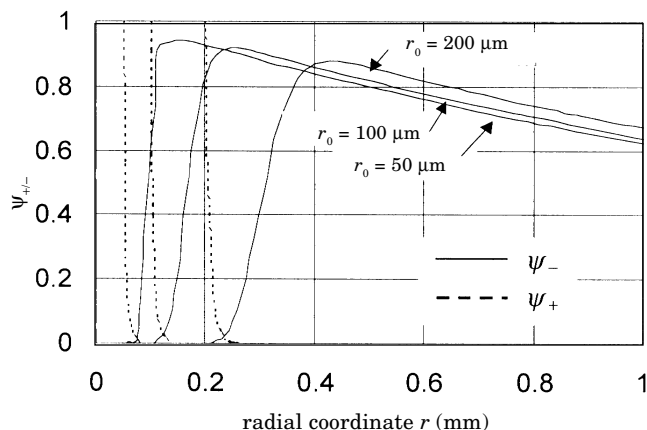


**Figure 5.** Distribution of the ratio of the electron current and the total current.

electrode. These characteristics are also similar to those of the corotron<sup>9</sup> and supported by the experimental results that the thickness of luminescence in negative discharging was about 0.1 mm<sup>20</sup> and larger than in positive discharging.<sup>19</sup>

### Ozone Generation Rate

Figure 7 shows the relationship between the radius of the discharge electrode and the ozone generation rate. The experimental data in this figure were adopted from Refs. 13, 18, and 19. Because the ozone generation rate is assumed to be almost linear with respect to the discharge current, averaged rates of experimental data were plotted in Fig. 7. Furthermore experimental values were normalized at the conditions of 20°C temperature, zero humidity, and 3 m/s air flow velocity using experimental data on the influences of these factors.<sup>18,21</sup> The results of the investigation show the following:

1. The calculated rate of the ozone emission by the negative discharge agreed fairly well with experiments. However, a substantial difference existed in the positive discharge, especially in larger diameter electrodes. The reason of the discrepancy is not clear but a similar characteristic is reported in the corotron.<sup>9</sup> According to Nashimoto's report,<sup>7</sup> the ozone formation in corotron is affected by materials used for the discharging wire electrode, especially in the case of the positive corona. This is because ozone is formed at the surface of the positive electrode, as shown in Fig. 6, and, as experimentally indicated, the ozone formation is highly dependent on  $\Delta H_0$  (the highest standard heat of formation of oxides per oxygen atom) of the discharge electrode. In the case of a negative corona, on the other hand, ozone is formed apart from the discharge electrode and hence it shows little dependence on  $\Delta H_0$ . Further experiments are necessary to prove this hypothesis in the pin-to-plate system.
2. The rate of the ozone emission by negative discharge is several times larger than that by positive discharge.
3. The ozone emission is smaller at a thinner discharge electrode.

Nashimoto<sup>7</sup> also qualitatively discussed characteristics 2 and 3 for corotrons and assumed that the genera-

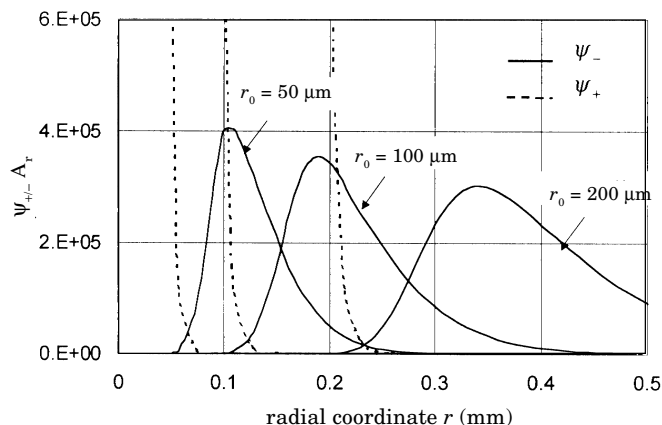


**Figure 6.** Distribution of ozone generation rate.

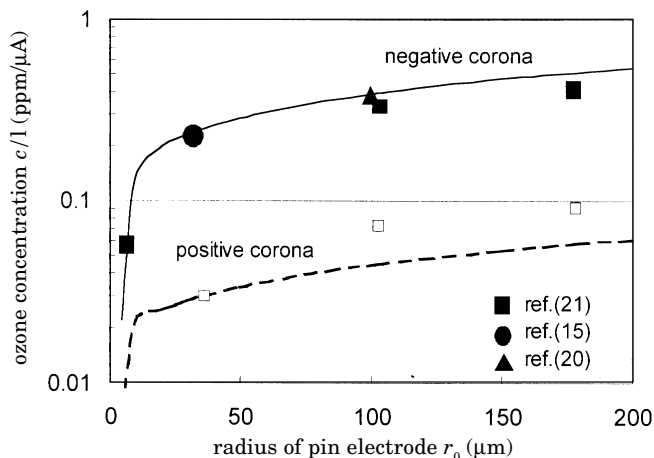


**Figure 7.** Measured and calculated ozone generation rate ( $Q = 1.5$  liter/min).

tion of ozone proportionally increases with an increase of the corona plasma volume around the discharge electrode. The present model also quantitatively supports this hypothesis.

### Comparison with Corotron and Biased Contact Roller

The calculated ozone concentration is 63 ppm at 5 liter/min air flow rate for the corotron of a 30  $\mu\text{m}$  radius wire made of tungsten under 400  $\mu\text{A}$  total current which corresponds to the current to charge the typical photoreceptor of a low-speed (11 A4/min) A4-width laser printer.<sup>11</sup> It can be reduced to 1.4 ppm by adopting a biased contact roller.<sup>11</sup> On the other hand, it is only 0.46 ppm at the same condition for the charger with saw-tooth electrodes. The rate of ozone emission can be drastically reduced by use of the proposed charging system.

### Concluding Remarks

A theoretical investigation has been performed to clarify ozone formation by the new electrophotography charger with saw-tooth electrodes. The following is a summary of the investigation.

## Characteristics

The rate of the ozone emission by negative discharge is several times larger than by positive discharge and in both cases the ozone emission is smaller at a thinner discharge electrode. This is because the generation of ozone proportionally increases with an increase of the corona plasma volume around the discharge electrode. It was confirmed by numerical calculation that plasma volume of the positive corona is smaller than that of the negative corona. In the case of the positive corona, ozone is formed just at the surface of the discharge electrode. On the contrary, in the case of the negative corona, ozone is formed about 0.1 mm away from the electrode. Although the rate of ozone emission is nonlinear with respect to the discharge current, it is approximately linear within the usual design and operation conditions of electrophotography chargers.

## Feasibility for Electrophotographic Charger

The ozone generation rate of the 50  $\mu\text{m}$  radius pin electrode is 0.085 ppm/ $\mu\text{A}$  under 5 liter/min air flow rate in case of negative corona. The ozone generation of the charger with saw-tooth electrodes is reduced to about one third of that with a biased charger roller, and it is only 1/140 of that with the corotron. The rate of ozone emission can be reduced drastically by use of the saw-tooth electrodes, compared with the corotron and the biased contact roller. The saw-tooth charger has a potential to realize a virtually ozone-free charger.  $\blacktriangle$

**Acknowledgment.** The author is grateful to Prof. Masui at Science University of Tokyo for valuable discussions.

This work is supported by The Iwatani Naoji Foundation's Research Grant.

## References

1. R. M. Schaffert, *Electrophotography*, 2nd ed., Focal Press, London, 1975.
2. S. Nakamura, H. Kisu, J. Araya, and K. Okuda, *Electrophoto.* **30**, 302 (1991).
3. J. Araya, N. Koitabashi, S. Nakamura, and H. Hirabayashi, *USP* 5,164,779 (1992).
4. J. Araya, N. Koitabashi, S. Nakamura, and H. Hirabayashi, *EP* 280 542 (1988).
5. S. Nakamura, *Electrophoto.* **30**, 312 (1991).
6. T. B. Hansen and B. Andersen, *Am. Ind. Hyg. Assoc. J* **47**, 659 (1986).
7. K. Nashimoto, *J. Imaging Sci. Technol.* **32**, 205 (1988).
8. G. V. Naidis, *J. Phys. D: Appl. Phys.* **25**, 477 (1992).
9. H. Kawamoto, *J. Imaging Sci. Technol.* **39**, 439 (1995).
10. H. Kawamoto and H. Satoh, *J. Imaging Sci. Technol.* **38**, 383 (1994).
11. H. Kawamoto, *J. Imaging Sci. Technol.* **39**, 267 (1995).
12. K. Furukawa, H. Ishii, K. Shiojima, and T. Ishikawa, *IS&T's Tenth Int. Congress on Advances in Non-Impact Printing Technologies*, IS&T, Springfield, VA, 1994, p. 34.
13. K. Furukawa, H. Ishii, K. Shiojima, and T. Ishikawa, *Electrophoto.* **35**, 116 (1996).
14. J. M. Meek and J. D. Craggs, Eds., *Electrical Breakdown of Gases*, John Wiley & Sons, 1978.
15. J. W. Gallagher, E. C. Beaty, J. Dutton, and L. C. Pichford, *J. Phys. Chem. Ref. Data* **12**, 109 (1983).
16. H. Kawamoto, *J. Imaging Sci. Technol.* **41**, 629 (1997).
17. M. Hattori and K. Asano, *T. IEE Japan* **106** A, 95 (1986).
18. K. Ohta, Y. Tanimura, N. Nakatsugawa, and A. Ikeda, *Proc. Inst. Electrostat. Jpn.* **20**, 42 (1996).
19. N. Masui, T. Yashima, T. Hamaguchi, Y. Murata, and T. Tani, *Proc. Inst. Electrostat. Jpn.* **22**, 98 (1998).
20. W. F. Lama and C. F. Gallo, *J. Appl. Phys.* **45**, 103 (1974).
21. K. Ikebe, K. Nakanishi and S. Arai, *T. IEE Japan* **109** A, 474 (1989).